



Constructing a molecular theory of self-assembly: Interplay of ideas from surfactants and block copolymers



Ramanathan Nagarajan

Natick Soldier Research, Development and Engineering Center, General Greene Avenue, Natick, MA 01760, United States

ARTICLE INFO

Available online 9 December 2016

Keywords:

Theory of surfactant and block copolymer micelles
Free energy model for micelles
Aggregate shape transitions
Head group repulsions and tail packing
Soluble block interactions and insoluble block deformation
Interfacial vs bulk control of solubilization

ABSTRACT

Low molecular weight surfactants and high molecular weight block copolymers display analogous self-assembly behavior in solutions and at interfaces, generating nanoscale structures of different shapes. Understanding the link between the molecular structure of these amphiphiles and their self-assembly behavior has been the goal of theoretical studies. Despite the analogies between surfactants and block copolymers, models predicting their self-assembly behavior have evolved independent of one another, each overlooking the molecular feature considered critical to the other. In this review, we focus on the interplay of ideas pertaining to surfactants and block copolymers in three areas of self-assembly. First, we show how improved free energy models have evolved by applying ideas from surfactants to block copolymers and vice versa, giving rise to a unitary theoretical framework and better predictive capabilities for both classes of amphiphiles. Second we show that even though molecular packing arguments are often used to explain aggregate shape transitions resulting from self-assembly, the molecular packing considerations are more relevant in the case of surfactants whereas free energy criteria are relevant for block copolymers. Third, we show that even though the surfactant and block copolymer aggregates are small nanostructures, the size differences between them is significant enough to make the interfacial effects control the solubilization of molecules in surfactant micelles while the bulk interactions control the solubilization in block copolymer micelles. Finally, we conclude by identifying recent theoretical progress in adapting the micelle model to a wide variety of self-assembly phenomena and the challenges to modeling posed by emerging novel classes of amphiphiles with complex biological, inorganic or nanoparticle moieties.

Published by Elsevier B.V.

1. Introduction

Surfactants and amphiphilic block copolymers display characteristic molecular self-assembly behavior in solutions, at interfaces and in bulk, generating nanoscale structures of different shapes. These nanoscale features determine many characteristics of these amphiphiles, relevant for their practical applications in materials, energy, consumer products, pharmaceutical and biomedical technologies. The ability to generate desired nanoscale morphologies by synthesizing novel amphiphiles so that the amphiphilic systems can be tailored for specific applications remains the long term goal of research in this field. Critical to achieving this goal is an understanding of the link between the molecular structure of the amphiphiles and their self-assembly behavior. In this review, we discuss the principles of self-assembly for both conventional low molecular weight surfactants and amphiphilic block copolymers focusing mainly on how model features developed independently for surfactants and block copolymers have been applied to one another, thereby capturing neglected factors influencing self-assembly. The similarity

and differences between the behavior of classical surfactants and amphiphilic block copolymers are identified.

Tanford [1] and Israelachvili, Mitchell and Ninham [2] pioneered two of the most important ideas that currently dominate our understanding of surfactant self-assembly. Tanford proposed the concept of opposing forces to formulate a quantitative expression for the standard free energy change on aggregation. In his model, the formation of the equilibrium aggregate resulted from balancing the interfacial free energy at the micelle-water interface against the repulsions between the surfactant head groups also located at the interface. Using this free energy expression, he was able to explain why surfactant aggregates form in aqueous solutions, why they grow, and why they do not keep growing but remain finite in size. Israelachvili, Mitchell and Ninham proposed the concept of a molecular packing parameter P and demonstrated how the size and the shape of the aggregate at equilibrium can be predicted from the magnitude of P in accordance with molecular packing considerations. It will be fair to assert that we can fully understand conceptually the molecular self-assembly principles governing surfactant behavior based on these two pioneering contributions.

Experimental and theoretical studies of self-assembly of block copolymers evolved without any obvious contact with the surfactant self-

E-mail address: Ramanathan.Nagarajan.Civ@mail.mil.

assembly literature. Theoretical understanding of how pure block copolymers organize into microdomains was advanced through the work of Meier [3,4] and Helfand [5,6]. Theoretical treatments of block copolymer micelles in selective solvents or in homopolymers have been pioneered by de Gennes [7], Leibler, Orland and Wheeler [8], Noolandi and Hong [9] and Whitmore and Noolandi [10]. de Gennes [7] analyzed the formation of a diblock copolymer micelle in selective solvents by minimizing the free energy per molecule of an isolated micelle with respect to the aggregation number or core radius. The micelle core was assumed fully segregated and devoid of any solvent. The free energy of formation of the core–corona interface and the elastic free energy of stretching of the core blocks control the micellization behavior. Leibler et al. [8] treated the problem of micelle formation of a symmetric diblock copolymer in a homopolymer solvent. In their study and in de Gennes' work, the interface was taken to be sharp. Noolandi and Hong [8] and Whitmore and Noolandi [9] formulated mean field models taking into account the possibility of a diffuse interface between the core and corona regions. In all treatments of block copolymer self-assembly, the elastic deformation of the core forming block played a central role. In the next section we outline the models for surfactants and block copolymers and then show how they borrowed from each other to account for missing effects thereby improving their quantitative predictive abilities.

2. Free energy model for micelles

2.1. Tanford model for surfactant micelles

Surfactant molecules self-assemble into spherical or cylindrical micelles or spherical bilayers, also known as vesicles (Fig. 1). The size and shape of the aggregates are dependent on the surfactant molecular structure as well as the solution conditions. Theoretical models in the literature have attempted to establish this interrelation. Tanford proposed the concept of opposing forces to formulate a quantitative expression for the standard free energy change on aggregation, $\Delta\mu_g^0$ [1, 11]. Here, $\Delta\mu_g^0 = \frac{\mu_g^0}{g} - \mu_1^0$, where μ_g^0 is the standard state chemical potential of an isolated micelle of aggregation number g while μ_1^0 is the standard state chemical potential of a singly dispersed surfactant, both in bulk solvent.

Tanford proposed that the standard free energy change is composed of three contributions:

$$\left(\frac{\Delta\mu_g^0}{kT}\right) = \left(\frac{\Delta\mu_g^0}{kT}\right)_{Tr} + \left(\frac{\Delta\mu_g^0}{kT}\right)_{Int} + \left(\frac{\Delta\mu_g^0}{kT}\right)_{Head} \quad (1)$$

Here, k is the Boltzmann constant and T is the temperature. The first term $(\Delta\mu_g^0/kT)_{Tr}$ is a negative free energy contribution arising from the

transfer of the tail from its unfavorable contact with water to the hydrocarbon-like environment of the aggregate core. This transfer free energy contribution depends on the surfactant tail but not on the aggregate shape or size. The second term $(\Delta\mu_g^0/kT)_{Int}$ provides a positive contribution that accounts for the fact that the entire surface area of the tail is not removed from water but there is still residual contact with water at the surface of the aggregate core. This is represented as the product of a contact free energy per unit area σ (or an interfacial free energy) and the surface area per molecule of the aggregate core, a . The third term $(\Delta\mu_g^0/kT)_{Head}$ provides another positive contribution to account for the repulsive interactions between the head groups that crowd at the aggregate surface. The repulsions are due to steric interactions (for any type of head group) and also electrostatic interactions (dipole–dipole interactions for zwitterionic head groups and ion–ion repulsions for ionic head groups). Since the repulsion would increase if the head groups come close to one another, Tanford proposed an expression for this free energy contribution with an inverse dependence on a . Thus, the standard free energy change per molecule on aggregation proposed by Tanford has the form:

$$\left(\frac{\Delta\mu_g^0}{kT}\right) = \left(\frac{\Delta\mu_g^0}{kT}\right)_{Tr} + \left(\frac{\sigma}{kT}\right)a + \left(\frac{\alpha}{kT}\right)\frac{1}{a} \quad (2)$$

where α is the head group repulsion parameter.

From the free energy model of Tanford, the equilibrium aggregation behavior can be examined either by treating the surfactant solution as consisting of aggregates with a distribution of sizes or by treating the aggregate as constituting a pseudophase. If the aggregate is viewed as a pseudophase, in the sense of small systems thermodynamics, the equilibrium condition corresponds to a minimum in the standard free energy change per molecule, $\Delta\mu_g^0/kT$. The minimization can be done with respect to either the aggregation number g or the core surface area per molecule a , since they are dependent on one another through the geometrical relations given in Table 1. One obtains in this manner, the equilibrium condition:

$$\frac{\partial}{\partial a} \left(\frac{\Delta\mu_g^0}{kT}\right) = \left(\frac{\sigma}{kT}\right) - \left(\frac{\alpha}{kT}\right)\frac{1}{a^2} = 0, \text{ at } a = a_e \Rightarrow a_e = \left(\frac{\alpha}{\sigma}\right)^{1/2} \quad (3)$$

The critical micelle concentration (cmc, denoted as X_C in mole fraction units), in the pseudophase approximation, is obtained from the relation,

$$\ln X_C = \left(\frac{\Delta\mu_g^0}{kT}\right)_{Tr} + \left(\frac{\sigma}{kT}\right)a_e + \left(\frac{\alpha}{kT}\right)\frac{1}{a_e} = \left(\frac{\Delta\mu_g^0}{kT}\right)_{Tr} + \left(\frac{2\sigma^{1/2}\alpha^{1/2}}{kT}\right) \quad (4)$$

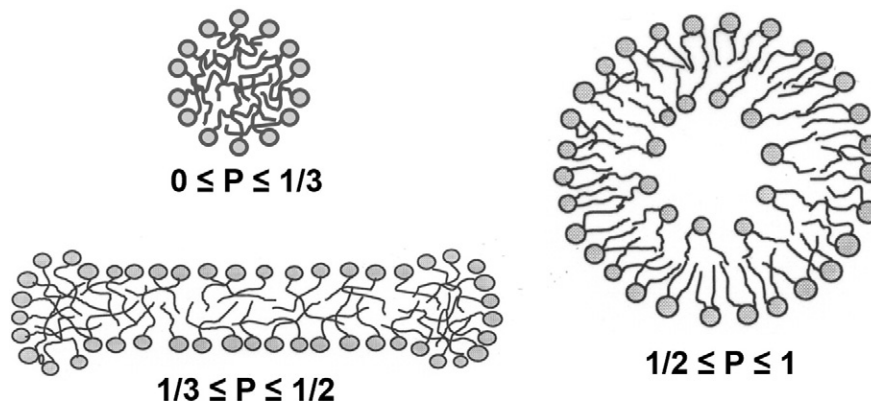


Fig. 1. Schematic representation of surfactant aggregates in dilute aqueous solutions. The structures formed include spherical micelles, spherical bilayer vesicles. One characteristic dimension in each of these aggregates is limited by the length of the surfactant tail. P is the molecular packing parameter discussed in Section 3.1 that determines the shape of the aggregate.

Table 1
Geometrical relations for spherical and cylindrical micelles and bilayers*.

Variable	Sphere	Cylinder	Bilayer
Volume of core $V = g v_o$	$4\pi R^3/3$	πR^2	$2R$
Surface area of core $A = g a$	$4\pi R^2$	$2\pi R$	2
Area per molecule a	$3v_o/R$	$2v_o/R$	v_o/R

* R is the core radius in case of spherical or cylindrical micelles and in the case of lamella, it is the half-bilayer thickness. g denotes the number of surfactant or block copolymer molecules in the aggregate. v_o is the volume and l_o is the extended length of the surfactant tail. The variables V, A , and g refer to the entire aggregate in the case of a sphere, unit length in the case of a cylinder or unit area in the case of a bilayer. The packing parameter P is defined as $P = v_o/a l_o$.

In Tanford free energy expression (Eq. (2)), the first contribution, the tail transfer free energy, is negative. Hence, this contribution is responsible for the aggregation to occur. It affects only the cmc (as shown by Eq. (4)) but not the equilibrium area a_e (as shown by Eq. (3)) which determines the size and shape of the aggregate. The second contribution, the free energy of residual contact between the aggregate core and water, is positive and decreases in magnitude as the area a decreases. A decrease in the area a , corresponds to an increase in the aggregation number g , for all aggregate shapes, as shown on Table 1. Hence, this contribution promotes the growth of the aggregate. The third contribution, the free energy due to head group repulsions, is also positive and increases in magnitude if the area a decreases or the aggregation number g increases. Hence, this contribution is responsible for limiting the growth of aggregates to a finite size. Thus, Tanford model clearly identifies why aggregates form, why they grow and why they do not keep growing but remain finite in size.

Tanford model explicitly attributes a central role to the surfactant headgroup in controlling self-assembly because the magnitude of head group repulsions determines the equilibrium area per molecule, and hence the size and shape of the surfactant aggregate. However, the surfactant tail influences only the magnitude of the cmc and has no role in determining the aggregate size or shape.

2.2. De Gennes model for block copolymer micelles

In contrast to the surfactant aggregates discussed above that are formed in water as the solvent, block copolymer micelles can be generated in any solvent as long as the solvent is non-selective to one block (solvophobic block denoted as A) and selective to the other block (solvophilic block denoted as B). The solvophobic block forms the core of the aggregate and the solvophilic block forms the shell or the corona of the aggregate. de Gennes [7] analyzed the formation of AB diblock copolymer micelles in a selective solvent by minimizing the free energy per molecule of an isolated micelle ($\Delta\mu_g^o$). The micelle core was assumed to be fully segregated, devoid of any solvent and the interface is treated as sharp. In de Gennes model, the free energy of formation of the micellar core–corona interface and the free energy of stretching of the solvophobic block constituting the micelle core control the micellization behavior.

The free energy model of de Gennes was written as

$$\begin{aligned} (\Delta\mu_g^o) &= (\Delta\mu_g^o)_{A,Tr} + (\Delta\mu_g^o)_{A,def} + (\Delta\mu_g^o)_{int} \\ (\Delta\mu_g^o) &= (\Delta\mu_g^o)_{A,Tr} + \frac{R^2}{N_A} + \sigma \frac{N_A}{R} \end{aligned} \quad (5)$$

The first term is the transfer of the solvophobic block A from the incompatible solvent to the micelle core resembling a melt of polymer block A. This term was not explicitly written in the original de Gennes paper but was obviously implied as it is the negative free energy contribution promoting self-assembly to occur. The second term is the stretching or elastic deformation of the solvophobic block A within the micelle core. The third term is the free energy of formation of the

interface between the micelle core and the corona region. The core block stretching is related to the core dimension and the number of segments N_A in the A block while the interfacial free energy is related to the area per molecule a , which is inversely related to the core radius R . Explicit expressions for each of the contributions are also shown in Eq. (5) in the spirit of scaling models, excluding any numerical coefficients and treating all variables as non-dimensional. In the last term accounting for the interfacial free energy, the relation between the area per molecule and core radius given in Table 1, $a \sim N_A/R$, has been used noting that the volume of block A is proportional to the number of segments N_A in the block. From the minimization of the free energy, the de Gennes model predicts that the micelle core radius R and the aggregation number g are related to the size N_A of the solvophobic block as $R \sim N_A^{2/3} \sigma^{1/3}$, $g \sim R^3/N_A \sim N_A \sigma$.

In the de Gennes free energy model, the solvophilic block B is considered to have no influence on the micelle characteristics and therefore the aggregate size has no dependence on the number of segments N_B in the B block. Note that the solvophilic block interactions in block copolymer micelles are analogous to the head group interactions in surfactant micelles. This offers a marked contrast to Tanford model for surfactants, where the head group repulsions were the principal contribution controlling the finite size of surfactant aggregates.

2.3. Star polymer model for block copolymer micelles

The solvophilic block B is recognized explicitly in the star polymer model for block copolymer micelles. The star polymer model for micelles is built upon the analogy between the conformation of star-shaped polymers and micelles. Star polymers resemble micelles, but for the important difference that a chemical link exists at the center between the various branches of the star polymer (Fig. 2). Daoud and Cotton [12] studied the conformation of a uniform star polymer, with g branches joining at the origin, present in a good solvent. They identified three distinct regions in this conformation—a swollen region, an unswollen region, and a uniform density region. For each of these three regions, they developed expressions for the radial concentration profiles utilizing the concept of blobs employed in theories of semidilute solutions of linear polymers. They also derived an expression for the

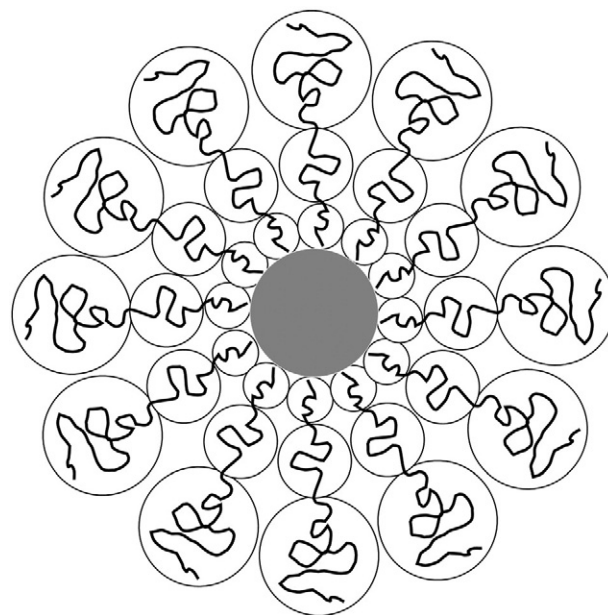


Fig. 2. Schematic representation of the star polymer model for the corona region of the block copolymer micelle. The uniform star is made of multiple branches all joining at the surface of the micelle core. Every branch is made of a succession of blobs whose size increases from the core surface to the outside. The free energy is simply equal to the number of blobs.

spatial extension of the branches as a function of the number of branches in the star polymer. These results from the Daoud-Cotton model are the basis of the scaling analysis of spherical and cylindrical micelles in good and theta solvents, pioneered by Zhulina and Birshtein [13] and the star model for spherical micelles in good solvents independently formulated by Halperin [14].

We have applied the Daoud-Cotton results to formulate a star polymer model for both micellization as well as solubilization [15] in block copolymer solutions. The development of various free energy contributions and the predictions for different cases of block composition, block size and solvent-block interactions are detailed in that study. Here, we will present only the final results from the star polymer model, focusing on the role of the soluble block. Therefore, the results are given only for the case when the selective solvent is a good solvent for the solvophilic block B, since this is the condition where we expect the solvophilic block interactions to be most important. As is conventional in scaling analysis, all numerical coefficients are ignored while writing various equations. All spatial variables such as the core radius R , the corona thickness D , the core area per molecule a , are expressed as dimensionless quantities and the free energy contributions are expressed in units of kT .

Based on the application of the star polymer concept, the free energy per molecule of the block copolymer micelle is written as

$$\begin{aligned} (\Delta\mu_g^0) &= (\Delta\mu_g^0)_{A,Tr} + (\Delta\mu_g^0)_{A,def} + (\Delta\mu_g^0)_B + (\Delta\mu_g^0)_{int} \\ (\Delta\mu_g^0) &= (\Delta\mu_g^0)_{A,Tr} + \frac{R^2}{N_A} + g^{1/2}K_B + \sigma \frac{N_A}{R}, \quad K_B = \ln\left(1 + \frac{D}{R}\right) \end{aligned} \quad (6)$$

Note that the free energy of transfer of the solvophobic block A from the incompatible solvent to the micelle core is usually not explicitly written but is obviously implied. This term provides the negative free energy contribution driving aggregate formation but is independent of the size and shape of the aggregate and therefore is not needed here. The core block elastic deformation and the interfacial energy term are as in the de Gennes model. The only new addition is the B block dependent term written here based on the blob picture of the star polymer model. We carry out free energy minimization for the limiting case when $(\Delta\mu_g^0)_B$ is dominant compared to $(\Delta\mu_g^0)_A$. When N_B is much larger than N_A , the shell block free energy contribution $(\Delta\mu_g^0)_B$ can be dominant compared to the core block free energy contribution $(\Delta\mu_g^0)_A$. One may note that when $N_B \gg N_A$, we have correspondingly $D/R \gg 1$. In this case we get,

$$\begin{aligned} R &\sim N_A^{3/5} \sigma^{2/5} K_B^{-2/5}, \quad g \sim N_A^{4/5} \sigma^{6/5} K_B^{-6/5}, \quad D \sim N_A^{4/25} N_B^{3/5} \sigma^{6/25} \omega_B^{1/5} K_B^{-6/5} \\ K_B &= \ln\left(1 + \frac{D}{R}\right) \approx \ln(D/R) \approx \ln\left(N_A^{-\frac{11}{25}} N_B^{\frac{3}{5}} \sigma^{-\frac{4}{25}} \omega_B^{\frac{1}{5}} K_B^{\frac{4}{25}}\right) \approx \ln\left(N_A^{-\frac{11}{25}} N_B^{\frac{3}{5}}\right) \end{aligned} \quad (7)$$

where $\omega_B = (1/2 - \chi_{BS})$ and χ_{BS} is the block B–solvent S Flory interaction parameter. We find the micelle core radius and aggregation number are only weakly influenced by the solvophilic block, with a logarithmic dependence on N_B (appearing through K_B). Certainly this is much weaker than the case of surfactant micelles where the head group interactions are paramount.

2.4. Surfactant micelle model borrows from block copolymer model

The block copolymer micelle model treats the elastic stretching of the solvophobic block as a key contribution to the micelle free energy while this contribution is not considered at all in the Tanford model for surfactants. Therefore, we borrow from the idea applied to block copolymer micelles and introduce this new contribution in the free energy model for surfactant micelle [16]. We formulated an analytical expression for the free energy of chain packing by adopting the treatment pioneered by Semenov [17] for block copolymer chain stretching in

confined geometries. The derivation of this expression takes into account the fact that the tail has to deform non-uniformly along its length to fill the aggregate core with uniform density.

The free energy model for surfactants, incorporating the contribution from tail packing (or elastic deformation) can be written as

$$\begin{aligned} \left(\frac{\Delta\mu_g^0}{kT}\right) &= \left(\frac{\Delta\mu_g^0}{kT}\right)_{Tr} + \left(\frac{\Delta\mu_g^0}{kT}\right)_{Int} + \left(\frac{\Delta\mu_g^0}{kT}\right)_{Head} + \left(\frac{\Delta\mu_g^0}{kT}\right)_{Pack} \\ \left(\frac{\Delta\mu_g^0}{kT}\right)_{Pack} &= \frac{3\pi^2}{80} \frac{R^2}{NL^2}, \quad \frac{5\pi^2}{80} \frac{R^2}{NL^2}, \quad \frac{10\pi^2}{80} \frac{R^2}{NL^2} \end{aligned} \quad (8)$$

The first three free energy contributions come from the original Tanford model while the fourth contribution for packing is borrowed from the block copolymer theory. The three expressions shown for packing free energy contributions are valid for spheres, cylinders and bilayers, respectively. In the packing free energy contribution, L is a characteristic segment length that is taken to be 4.6 Å (see Ref. [16] for details) and N is the number of segments in a tail such that $NL^3 = v_o$. Since $R = 3 v_o/a$, $2 v_o/a$, and v_o/a for the three geometries (Table 1), the packing free energy contribution can be rewritten as

$$\left(\frac{\Delta\mu_g^0}{kT}\right)_{Pack} = \frac{Q}{a^2}, \quad Q_{sph} = \frac{27}{8} v_o L, \quad Q_{cyl} = \frac{20}{8} v_o L, \quad Q_{bilayer} = \frac{10}{8} v_o L, \quad (9)$$

where the symbol Q is used to denote the coefficient of $1/a^2$ in the free energy expression and it stands for Q_{sph} , Q_{cyl} or $Q_{bilayer}$ depending upon the aggregate shape. The equilibrium area a_e given before by Eq. (3) is now obtained from the modified relation

$$\begin{aligned} \frac{\partial}{\partial a} \left(\frac{\Delta\mu_g^0}{kT}\right) &= \left(\frac{\sigma}{kT}\right) - \left(\frac{\alpha}{kT}\right) \frac{1}{a^2} - \frac{2Q}{a^3} = 0, \text{ at } a = a_e \Rightarrow a_e \\ &= \left(\frac{\alpha}{\sigma} + \frac{2Q/a_e}{\sigma/kT}\right)^{1/2} \end{aligned} \quad (10)$$

Since the variable Q is dependent on the tail, the tail has direct influence over the equilibrium area a_e and the packing parameter P . The consequence is the direct control exerted by the tail over the size and shape of the equilibrium aggregate.

Illustrative numerical calculations have been carried out taking into account this packing free energy contribution. For this purpose, we have chosen a value of $(\alpha/kT) = 500 \text{ \AA}^2$ for the head group interaction parameter and $(\sigma/kT) = 0.12 \text{ \AA}^{-2}$, consistent with σ being around 50 mN/m for aliphatic hydrocarbons–water interface. Q depends on the tail length as well as the shape of the aggregate within which the tails have to pack, as shown in Eq. (9).

A summary of the calculated results for three tail lengths of single tail surfactants is given in Table 2. Shown on the Table are the equilibrium area a_e calculated from the Tanford model (Eq. (3)) and the model influenced by block copolymers Eq. (10) that takes into account the elastic deformation of the surfactant tail. Since the Tanford model does not attribute any role for the surfactant tail in controlling the micelle size or shape, the calculated equilibrium area per molecule is independent of the tail length. In contrast, in the model that includes the hydrophobic tail stretching in the micelle core, the area per molecule shows a tail length dependence and increases as the tail length increases. One can observe that the effect is appreciable enough when it comes to

Table 2
Influence of surfactant tail deformation on micelle size for surfactants.

n_c	$v_o (\text{\AA}^3)$	$Q_{sph} (\text{\AA}^4)$	$a_e (\text{\AA}^2)$ (from Eq. (3))	$a_e (\text{\AA}^2)$ (from Eq. (10))
8	243	3773	64.5	71.1
12	351	5449	64.5	73.5
16	459	7126	64.5	75.8

considering the aggregation number of spherical micelle, but as will be shown below, it has even more critical impact on determining the shape of surfactant aggregates.

2.5. Block copolymer micelle model borrows from surfactant model

The surfactant micelle model treats the repulsive interactions between the hydrophilic head groups as a central contribution to the micelle free energy. Indeed, without this contribution finite micelles cannot be realized. In block copolymers, an analogous free energy contribution should arise from the difference in state of the hydrophilic block when the singly dispersed copolymer becomes part of the micelle. However, this contribution is not considered at all in the free energy model of de Gennes. While the star polymer model considered the B block dependent free energy, it did not yield a significant dependence of the micelle characteristics on the B block but only a weak logarithmic dependence. Therefore, we borrow from the surfactant model and introduce this new contribution in the model for block copolymers, using a mean field description for the free energy contribution [18–20]. The free energy model of de Gennes (Eq. (5)) is now modified to include the osmotic (dilution term) and elastic (deformation term) free energy contributions associated with the B block, equivalent to the head group repulsions for surfactants.

The free energy model for block copolymer micelles incorporating the solvophilic block interactions has the form

$$\begin{aligned} \left(\Delta\mu_g^0\right) &= \left(\Delta\mu_g^0\right)_{A,Tr} + \left(\Delta\mu_g^0\right)_{A,def} + \left(\Delta\mu_g^0\right)_{int} + \left(\Delta\mu_g^0\right)_{B,dil} + \left(\Delta\mu_g^0\right)_{B,def} \\ \left(\frac{\Delta\mu_g^0}{kT}\right)_{A,def} &= q \frac{p\pi^2}{80} \frac{R^2}{(N_A/q)L^2} \\ \left(\frac{\Delta\mu_g^0}{kT}\right)_{int} &= \frac{\sigma}{kT} a, \quad \sigma = \frac{kT}{L^2} \left(\frac{\chi_{AS}}{6}\right)^{1/2} \\ \left(\frac{\Delta\mu_g^0}{kT}\right)_{B,dil} &= N_B \frac{v_B}{v_s} \frac{1-\varphi_B}{\varphi_B} \ln(1-\varphi_B) + \frac{v_B}{v_s} (1-\varphi_B) \chi_{BS} \\ \left(\frac{\Delta\mu_g^0}{kT}\right)_{B,def} &= \frac{3}{2} \frac{LR}{\left(\frac{a}{q}\right)\varphi_B} \end{aligned} \quad (11)$$

Eq. (11) is written as to be valid for AB diblock and symmetric BAB triblock copolymers. In the A block elastic energy contribution, $q = 1$ for AB diblock and 2 for BAB triblock copolymers and $p = 3$ for spheres, 5 for cylinders, and 10 for lamella. In the B block deformation term based on the approach developed by Semenov [17], $P = (D/R)/(1 + D/R)$ for spheres, $P = \ln(1 + D/R)$ for cylinders and $P = (D/R)$ for lamellae [19,20]. The Semenov treatment accounts for the fact that the chain deformation has to be non-uniform in order to maintain uniform concentrations of segments in the corona region. We note in passing that in our first model for block copolymer micelles [18], we had used the Flory model for chain elasticity that assumes uniform chain deformation to calculate the deformation free energy contribution. Although the difference between estimates of the free energy from Flory and Semenov approaches is not too large [19], it is nevertheless pertinent for quantitative predictive purposes. The variables χ_{AS} and χ_{BS} denote the Flory interaction parameters of the A and the B block with solvent S, L is the characteristic segment size and φ_B is the volume fraction of polymer B segments in the corona region. In Eq. (11), we have not included any of the constant terms representing singly dispersed block copolymer state since they do not affect the size and shape of aggregates.

This free energy model is applicable to aggregates having spherical, cylindrical and lamellar (or bilayer) morphologies. All the geometrical properties of the aggregates appearing in the free energy expressions are summarized in Table 3. Note that in our detailed treatment of

Table 3
Geometrical relations for block copolymer aggregates.

Property	Sphere	Cylinder	Lamella
Core volume $V_C = g N_A v_A$	$4\pi R^3/3$	πR^2	$2R$
Corona volume V_S	V_C	V_C	V_C
	$[(1 + D/R)^3 - 1]$	$[(1 + D/R)^2 - 1]$	$[(1 + D/R) - 1]$
Aggregation number g	$V_C/(N_A v_A)$		
Core surface area/molecule a	$3 N_A v_A/R$	$2 N_A v_A/R$	$N_A v_A/R$
Volume fraction of B in corona φ_B	$(g N_B v_B)/V_S = (N_B v_B/N_A v_A)(V_C/V_S)$		

block copolymer micelles [18–20], we have also included a free energy contribution to account for the localization of the AB joint to a narrow volume of the aggregate and also a contribution that accounts for backfolding in the case of a BAB triblock copolymer. Both of these contributions are practically independent of the aggregate size and shape and therefore not shown in Eq. (11).

The symbols v_A and v_B refer to the molecular volumes of A and B segments, v_s is the molecular volume of the solvent, N_A and N_B are the number of segments of blocks A and B for both AB diblock and symmetric BAB triblock copolymers. The number of block copolymer molecules g in an aggregate, the aggregate core volume V_C , and the corona volume V_S all refer to the total quantities in the case of spherical aggregates, quantities per unit length in the case of cylindrical aggregates and quantities per unit area in the case of lamellar aggregates.

For illustrative purposes, calculations have been carried out [18] for the diblock copolymers polystyrene-polyisoprene (PS-PI) in n-heptane, which is a selective solvent for the PI block and non-selective for the PS block. The predicted aggregate core radius, corona thickness and aggregation number for spherical micelles are shown on Table 4 where the predictions are shown to compare reasonably against the experimental measurements reported [21] in the literature.

The PS-PI system discussed in Table 4 has a constant solvophilic block size. Since the solvophilic block effect is the new contribution introduced in the block copolymer model by borrowing ideas from the surfactant model, we have also carried out predictive calculations for different block sizes of the solvophilic block PB in the case of polystyrene-polybutadiene (PS-PB) micelles in n-heptane which is a selective solvent for PB [18]. The calculated results are summarized in Table 5.

Scaling relations between micellar size characteristics and the block sizes N_A and N_B have been obtained by correlating the experimental results for PS-PI-heptane and the calculated results for PS-PB-heptane,

$$R \sim N_A^{0.70} N_B^{-0.08}, \quad g \sim N_A^{1.10} N_B^{-0.24}, \quad D \sim N_A^{0.07} N_B^{0.68} \quad (12)$$

The core radius and the aggregation number show dependence on the solvophilic block B that was entirely absent in the case of de Gennes model and was much weaker in the case of the star polymer model. Indeed, the analog of surfactant head group repulsions is quite important for block copolymer micelles. Note that for both solvophilic blocks polyisoprene and polybutadiene, the solvent n-heptane is close to a theta solvent under the conditions examined. One can expect the B block

Table 4
Micellization of PS-PI in n-heptane at 25 °C.

N_B	N_A	R (Å)	D/R	g	R (Å)	D/R	g
PI block	PS block	Mean field model predictions			Experimental (19)		
295	86	85	1.77	187	94	1.77	248
295	156	128	1.24	352	119	1.31	278
295	184	144	1.12	422	141	1.13	386
295	278	193	0.87	672	194	0.96	666
295	316	211	0.80	778	240	0.92	1113

Table 5
Model predictions of micelles of PS-PB in n-heptane at 25 °C.

N_A PS block	N_B PB block	R (Å)	D/R	g
98	36	143	0.37	512
98	111	130	0.96	381
98	350	119	2.22	291
98	463	117	2.65	278
311	350	263	1.14	1005
538	350	390	0.80	1889
790	350	517	0.61	2985

dependent free energy contribution to gain greater importance when the selective solvent changes from being a theta solvent to a good solvent for the B block. Therefore we have considered PEO-PPO block copolymers aggregating in water, with water being a good solvent for the PEO block. Our calculations for PEO-PPO block copolymer micelles considering uniform concentration in the corona and uniform chain stretching for the coronal B block (Flory approach) yielded [18] the following scaling relations:

$$R \sim N_A^{0.73} N_B^{-0.17}, \quad g \sim N_A^{1.19} N_B^{-0.51}, \quad D \sim N_A^{0.06} N_B^{0.74} \quad (13)$$

showing much stronger dependencies on N_B compared to that seen for the theta solvent in Eq. (12). As mentioned earlier, maintaining uniform concentration in the corona would require non-uniform deformation of the coronal block B, we have applied the Semewnov approach and the corresponding model Eq. (11) to make predictions [22] for a wide range of PEO and PPO block sizes and those results are summarized in Table S1 of the Supplemental Information. By correlating the predicted results, we find the following scaling relations for the PEO-PPO-water system:

$$R \sim N_A^{0.73} N_B^{-0.29}, \quad g \sim N_A^{1.19} N_B^{-0.87}, \quad D \sim N_A^{0.06} N_B^{0.60} \quad (14)$$

One can observe the even stronger dependence of R and g on the size of the solvophilic block B predicted by the non-uniform chain deformation model compared to Eq. (13) based on the uniform chain deformation model. Therefore the free energy contributions analogous to surfactant head group repulsions are very important for block copolymers and the contribution leads to stronger dependencies on the B block when the selective solvent is a very good solvent for the B block.

3. Aggregate shape transitions

3.1. Shape transitions controlled by packing considerations for surfactants

The rationalization of why surfactant molecules choose to self-assemble as spherical micelles, cylindrical micelles or spherical bilayer vesicles was a fundamental problem in early surfactant theories. In surfactant aggregates, the hydrophobic domain is made up of the surfactant tails. If the density in the domains is considered equal to that in similar hydrocarbon liquids, the surfactant tails must entirely fill the space in these domains. As a result, irrespective of the shape of the aggregate, no point within the aggregate can be farther than ℓ_o from the aggregate-water interface, where ℓ_o is the extended length of the surfactant tail. Therefore, at least one dimension of the surfactant aggregates should be smaller than or at most equal to $2\ell_o$ [1]. This is purely a geometrical or packing constraint that the surfactant aggregate will have to satisfy [1,2].

The core volume is determined by the number of surfactant molecules in the aggregate and the volume of the surfactant tail. For a spherical micelle of core radius R , made up of g molecules, the volume of the core $V = g v_o = 4\pi R^3/3$, the surface area of the core $A = g a = 4\pi R^2$, and hence $R = 3 v_o/a$, from simple geometry (Table 1). If the micelle core is packed with surfactant tails without any empty space, then the radius R

cannot exceed the extended length ℓ_o of the tail. Introducing this constraint in the expression for R , one obtains the constraint, $0 \leq v_o/a\ell_o \leq 1/3$, for spherical micelles. This dimensionless group $v_o/a\ell_o$ is well-known as the molecular packing parameter P , first explicitly introduced by Israelachvili, Mitchell and Ninham [2]. The geometrical relations for aggregates given in Table 1, together with the constraint on one dimension of the aggregate, lead to the well-known [2] connection between the molecular packing parameter and the aggregate shape: $0 \leq v_o/a\ell_o \leq 1/3$ for sphere, $1/3 \leq v_o/a\ell_o \leq 1/2$ for cylinder, and $1/2 \leq v_o/a\ell_o \leq 1$ for bilayer. Note that the free energy plays a fundamental role, as it should, in determining the magnitude of the packing parameter, because the equilibrium area per molecule a_e is obtained from the condition of minimum free energy. However, the aggregate shape transitions are controlled by the packing constraint that results from the limit imposed on one dimension of the aggregate by the extended length of the surfactant molecule. In other words, for a given surfactant tail length (say 12 carbon atoms), there is a maximum number of surfactant molecules that can be incorporated within a spherical micelle (about 54) and the spherical shape is not viable if more surfactant molecules have to become part of the aggregate.

To compare the Tanford model (Eq. (3)) against the modified model Eq. (10) which incorporates ideas borrowed from the block copolymer theory, we provide some model predictions [23] for aggregate shape transitions for surfactants in Table 6. The calculations have been performed for a surfactant with a dodecyl alkane tail. As mentioned earlier, $(\sigma/kT) = 0.12 \text{ \AA}^{-2}$, consistent with σ being around 50 mN/m for the aliphatic hydrocarbon-water interface. The head group interaction parameter α/kT is taken as a variable in the range 500 \AA^2 to 60 \AA^2 to reflect the condition where the head group repulsions are decreased by adding salt to an ionic surfactant solution.

The inclusion of the packing free energy (Eq. (10)) by borrowing from block copolymer model, results in the equilibrium area a_e for surfactant aggregates being larger than that estimated from Eq. (3) neglecting this contribution. Since in all cases the area per molecule is increased, it implies that for any aggregate shape the modified model will predict a smaller aggregation number. More importantly, the change in predicted equilibrium area changes the predicted packing parameter as well. Therefore, the predictions of shape transitions are altered because of the consideration of the tail elastic stretching, so that spheres are preferred over cylinders at $\alpha/kT = 300 \text{ \AA}^2$ and cylinders are preferred over bilayer for $\alpha/kT = 120 \text{ \AA}^2$.

3.2. Shape transitions controlled by free energy considerations for block copolymers

Block copolymer aggregates also exist as spheres, cylinders or bilayers. The aggregation behavior diblock copolymers PEO-PPO of various molecular weights and compositions have been calculated [22] based on the mean field model (Eq. (11)) and the results are summarized in Table 7. The number of ethyleneoxide (EO) units in the PEO block and the propyleneoxide (PO) units in the PPO block are identified in Table 7 for each block copolymer. Considering block copolymers which have similar hydrophobic block lengths (EO₁₆PO₅₀ and EO₂₆₆PO₅₀, or EO₁₂PO₃₅, EO₁₈PO₃₂ and EO₄₅PO₃₅, for example) the core radius of the sphere is larger than the core radius of the cylinder, which in turn is larger than the half-bilayer thickness of the bilayer.

Table 6
Predicted aggregate shape transitions for surfactant with dodecyl tail.

α/kT (Å ²)	a_e (Å ²) Eq. (3)	$v_o/a_e\ell_o$ Eq. (3)	Shape Eq. (3)	a_e (Å ²) Eq. (10)	$v_o/a_e\ell_o$ Eq. (10)	Shape Eq. (10)
500	64.5	0.326	Sphere	73.5	0.286	Sphere
300	50.0	0.42	Cylinder	62.9	0.333	Sphere
240	44.7	0.47	Cylinder	56.5	0.372	Cylinder
120	31.6	0.664	Bilayer	48.8	0.430	Cylinder
60	22.4	0.938	Bilayer	37.4	0.561	Bilayer

Table 7
Predicted aggregate shape transitions for PEO-PPO diblock copolymer*.

Block copolymer	R (Å)	D (Å)	a_e (Å ²)	g	Aggregate Shape
EO ₁₆ PO ₅₀	32.6	21.9	148	1.35	Lamella
EO ₂₆₆ PO ₅₀	40.0	126	362	56	Sphere
EO ₁₂ PO ₃₅	26.2	17.3	129	1.55	Lamella
EO ₁₈ PO ₃₂	40.2	22.7	154	16.5	Cylinder
EO ₄₈ PO ₃₅	48.9	45.6	207	145	Sphere
PO ₁₀₄ PO ₃₅	39.3	72.7	258	75	Sphere

* g is the aggregation number defined as the total number of molecules in a micelle in the case of sphere, the number of molecules per nm length in the case of cylinder and the number of molecules per nm² area in the case of lamella.

This prediction is the direct result of the chain elastic deformation free energy contribution.

The shape transition of block copolymer aggregates as a function of the block copolymer composition shown on Table 7 follows the behavior exhibited by surfactant aggregates as a function of head group repulsions. For surfactants, when the head group repulsions are weak, lamellar aggregates are favored while for strong head group repulsions, spherical micelles are formed. Cylindrical micelles result for intermediate values of head group repulsions. For the block copolymer aggregates, the free energy contributions associated with the hydrophilic B domain are analogous to the head group repulsions in surfactant micelles. Therefore the pattern of aggregation observed for increasing head group repulsions in surfactants is exactly reproduced with increasing size of the hydrophilic block in the case of block copolymers. This has given rise to the notion [24,25] that the packing parameter P can be used to describe the shape transition of block copolymer aggregates (Fig. 3). For surfactants $P = v_0/a_e l_o$ and although the free energy determines the equilibrium area a_e , the constraint that the radius of spherical or cylindrical micelle or half bilayer thickness cannot exceed l_o plays a controlling role in influencing shape transitions. As mentioned earlier, a surfactant with a dodecyl tail can accommodate only 54 or fewer molecules if the aggregate shape is to remain spherical. However, in the case of the block copolymer, there is no equivalent constraint imposed by the extended length of the hydrophobic block. For example, if we look at the family of block copolymers in Table 8 with approximately 35 PO units, the extended length of the hydrophobic PPO block can be estimated roughly to be 161 Å, taking the segment length to be about 4.6 Å [26]. Corresponding to this extended length, spherical aggregates having a PO₃₅ core block can accommodate as many as 5175 molecules. However the calculations show that we form spherical micelles of core radius 49 Å and aggregation number 145 for EO₄₈PO₃₅. When the PEO chain length is decreased keeping the same hydrophobic block, even though there are no packing constraints that would prevent the sphere from

Table 8
Solubilization capacity of block copolymer micelles for hydrocarbons at 25 °C.

Solubilize	Molecular properties of solubilizes			mmoles solubilize per gram of core block		
	v_0 Å ³	σ_{ow} mN/m	δ_o MPa ^{1/2}	PEO-PPO	PVP-PS	SDS
Benzene	146	33.93	18.80	11.67	30	9.9
Toluene	176	36.1	18.19	6.33	14.8	8
O-Xylene	200	36.1	18.40	4.0	31.6	4.43
Ethyl Benzene	204	38.4	17.99	5.67	26.7	–
Cyclohexane	179	50.2	16.76	1.97	3	4.6
Hexane	217	50.7	14.92	0.667	0.77	2.39
Heptane	243	51.2	15.13	0.567	0.47	–
Octane	270	51.5	15.53	0.5	0.18	–
Decane	323	52	15.74	0.387	0.072	1.18

growing from 145 molecules all the way up to 5175 molecules, the micelle does not grow retaining spherical shape but changes to a cylinder for EO₁₈PO₃₂ and bilayer for EO₁₂PO₃₅. The predicted core radii are only 26 Å, 40 Å and 49 Å for EO₁₂PO₃₅, EO₁₈PO₃₂, and EO₄₈PO₃₅ block copolymers forming lamellar, cylindrical and spherical aggregates, much smaller than the extended length for the PPO block. Therefore, the shape transitions are not at all affected by any packing constraints imposed by the length of the hydrophobic block, a behavior different from that of the surfactants. The shape transitions occur because the free energy change ($\Delta\mu_g^0$) for cylinder becomes smaller than that for spheres and for the lamella becomes smaller than that of the cylinder as the PEO chain length decreases. In this sense, the free energy criterion completely controls the shape transition of block copolymer aggregates. Although cartoons such as in Fig. 3 can be used to qualitatively indicate how the balance between the hydrophobic and hydrophilic block sizes affect the aggregate shape transition, there is no quantitative support to using packing parameter as a model since extended length of the hydrophobic block cannot be used to calculate P for predictive purposes.

4. Solubilization in micelles

4.1. Solubilization controlled by interfacial interactions in surfactant micelles

The solubilization of hydrocarbons in micelles is a fundamental phenomenon that serves as the basis of numerous practical applications of surfactants. It was found that for a homologous family of aliphatic and aromatic solubilize molecules, the molar solubilization ratio (MSR) in the micelle (the ratio of the number of solubilize molecules to the number of surfactant molecules) decreases with increasing size of the

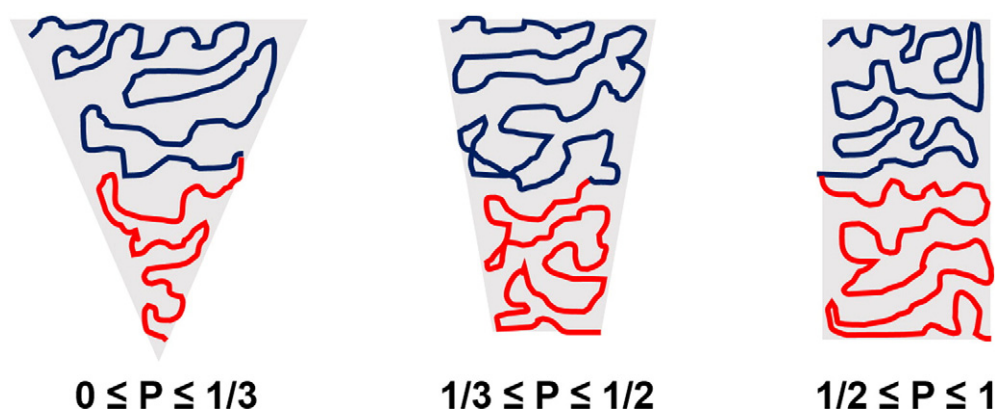


Fig. 3. Schematic of how molecular packing model for surfactants is considered applicable to block copolymers. The packing parameter P is shown to change depending upon the relative sizes of the solvophobic and solvophilic blocks of the copolymer. As discussed in the text, it is not obvious how the packing parameter can be calculated since the hydrophobic block (the analog of surfactant tail) typically has very long extended lengths and consequently does not impose any molecular packing constraints for spherical, cylindrical or lamellar aggregates generated by the block copolymer.

solubilize molecule [27]. Further, the aromatic molecules are solubilized to a larger extent than the aliphatic molecules of comparable molecular volume. Experimentally determined MSR for three ionic surfactants are listed in Table S2 of Supplemental Information.

To interpret these experimental results qualitatively, we adapt the Tanford model (Eq. (2)) for micelles to account for solubilization in the form

$$\left(\frac{\Delta\mu_g^0}{kT}\right) = \left(\frac{\Delta\mu_g^0}{kT}\right)_{Tr} + \left(\frac{\sigma + \Delta\sigma}{kT}\right)(a + \Delta a) + \left(\frac{\alpha}{kT}\right)\frac{1}{a + \Delta a} + \left(\frac{\Delta\mu_g^0}{kT}\right)_{Mix} \quad (15)$$

Three modifications have been introduced: (i) the area per molecule a in solubilize-free micelles is increased by an increment Δa to account for the swelling of the micelle core due to solubilize, (ii) the hydrocarbon tail-water interfacial tension σ is altered by an amount $\Delta\sigma$ to account for any changes in the tension that could be induced by the solubilize, and (iii) the mixing free energy of the solubilize with the surfactant tails is included. For aliphatic hydrocarbon solubilizes that have the same interfacial tension against water as the surfactant tail, $\Delta\sigma = 0$ and equilibrium will correspond to a fixed value of Δa or alternately a fixed increase in the core volume, irrespective of the molecular volume of the solubilize. This explains the experimental observation why the number of molecules solubilized per surfactant molecule (molar solubilization ratio) will be smaller if the molecular volume of the solubilize is larger. Now if we consider an aliphatic hydrocarbon and an aromatic hydrocarbon of equal molecular size, in the case of the aromatic hydrocarbon one can expect $\Delta\sigma < 0$, since the aromatic hydrocarbons have lower interfacial tension against water. Implicit in such consideration is the idea that the aromatic hydrocarbons can be in the proximity of the core-water interface to influence the effective micelle core - water interfacial tension. Therefore, for the same free energy change, it would be possible for Δa to be larger in the case of the aromatic hydrocarbon solubilize compared to the aliphatic hydrocarbon solubilize. This explains the experimental observation of why aromatic hydrocarbons will be solubilized more compared to aliphatic hydrocarbons of equal molecule size.

Based on the interpretation provided by Eq. (15) for solubilization, the experimental molar solubilization ratio for aliphatic and aromatic hydrocarbons have been correlated [27] to the molecular properties of the solubilizes:

$$MSR = a \left(\frac{\sigma_{ow} v_o^{2/3}}{kT}\right)^{-b} \quad (16)$$

Here, a and b are positive constants dependent on the surfactant molecule, σ_{ow} is the solubilize-water interfacial tension reflecting the interfacial activity of the solubilize and v_o is the molecular volume of the solubilize. From the experimental data (Fig. 4) we determine that the coefficient a in the correlation has the value 22.9 for cetyl pyridinium chloride (CPC), 29.5 for dodecyl ammonium chloride (DAC), and 13.2 for sodium dodecyl sulfate (SDS). For all three surfactants, the exponent b in the correlation has the value 2.3. The smaller the molecular volume and the larger the interfacial activity (indicated by a smaller value for σ_{ow}), the smaller is the volume-interfacial activity parameter and the larger the molar solubilization ratio. These results confirm that the interfacial interactions control the solubilization behavior in surfactant micelles. This is not surprising considering that the micelle core radius is typically in the range 10 Å to 20 Å for all classical surfactants and for purely geometrical size arguments, the solubilize molecules will have to be present near the core surface thereby influencing the interfacial interactions.

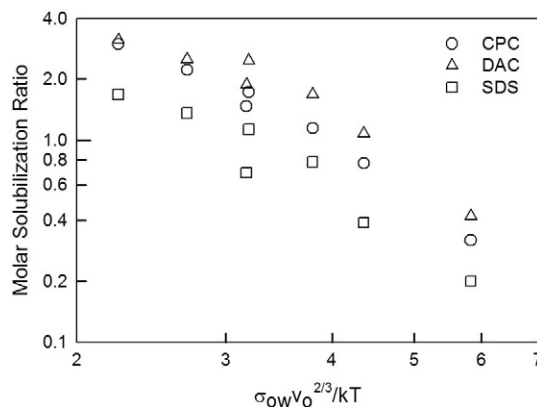


Fig. 4. Measured molar solubilization ratio [27] for aliphatic and aromatic hydrocarbons in ionic micelles of cetyl pyridinium chloride (CPC), dodecyl ammonium chloride (DAC) and sodium dodecyl sulfate (SDS). The molar solubilization ratio is correlated against the interfacial activity-volume parameter representing the solubilize molecules. The numerical data plotted here are listed in Table S2 of the Supplemental Information.

4.2. Solubilization controlled by bulk interactions in block copolymer micelles

The solubilization capacities for aromatic and aliphatic hydrocarbons have been determined also in block copolymer micelles [28] and the results are summarized in Table 8. The block copolymer molecules employed were PEO-PPO-PEO symmetric triblock copolymer F127 (EO₁₀₀PO₆₄EO₁₀₀) and polyvinyl pyrrolidone-polystyrene (PVP-PS) block copolymer of unspecified molecular weight with 60 wt% polystyrene. Also shown for comparison are the results for the surfactant SDS.

The amount of solubilization is expressed as mmoles solubilize per gram of the hydrophobic block of the copolymer or of the surfactant tail. The measurements show that aromatic hydrocarbons are solubilized more than aliphatic hydrocarbons. This is similar to the results discussed for surfactant micelles. Remarkably, all aromatic hydrocarbons are solubilized to a very large extent in the PVP-PS block copolymer whereas in the surfactant SDS, the amount solubilized decreased with increasing molecular volume of the solubilize. At the same time, all aliphatic hydrocarbons are solubilized to a much lower extent in the PVP-PS block copolymer compared to the surfactant SDS. Both the increase in the amount solubilized for aromatics and the decrease in the amount solubilized for aliphatics causes the selectivity to be significantly increased in the PVP-PS block copolymer compared to the surfactant SDS. The 4-fold difference between the solubilized moles of benzene and hexane in the surfactant SDS is replaced by a 17-fold difference in the PEO-PPO-PEO block copolymer and by a 40-fold difference in the PVP-PS block copolymer.

We note that aromatic hydrocarbons are good solvents for the PS block while aliphatic hydrocarbons are poor solvents for PS. Since the solvency of the blocks is represented quantitatively by the Flory polymer-solvent interaction parameter [29], one can look for a correlation between the solubilization capacity in block copolymer micelles and the Flory parameter describing core block-solubilize interactions. Table 8 lists some important molecular characteristics of the solubilizes: molecular volume (v_o), interfacial tension against water (σ_{ow}), and Hildebrand-Scatchard solubility parameter (δ_o) values [20]. The subscript o denotes the solubilize and w refers to water. The Flory interaction parameter χ_{AO} is calculated using the Hildebrand solubility parameters via the relation $\chi_{AO} = (\delta_A - \delta_o)^2 v_o / kT$, where δ_A is the solubility parameter for the A block. Taking δ_A to be 19 MPa^{1/2} for PPO, 18.6 MPa^{1/2} for PS, and 15.94 MPa^{1/2} for the dodecyl tail of the SDS, and using the molecular properties of solubilizes listed in Table 8, we can calculate the Flory interaction parameters for all the solubilizes [28] interacting with the different core blocks (PPO, PS and dodecyl

alkane tail in the case of SDS). The experimental solubilization data are correlated via the relation

$$MSR = a \chi_{AO}^{-b} = a \left[\frac{v_O(\delta_A - \delta_O)^2}{kT} \right]^{-b} \quad (17)$$

for both PEO-PPO-PEO and PVP-PS block copolymers. Here, MSR is the molar solubilization ratio (moles of hydrocarbon solubilized per mole of block copolymer), and a and b are positive constants that depend on the block copolymer molecule. The smaller the magnitude of the Flory interaction parameter, the better is the solubilize for the core block and higher the molar solubilization ratio.

This correlation has been confirmed in another comprehensive experimental study of solubilization of various organic molecules in polystyrene-polymethacrylic acid (PS-PMA) block copolymer micelles [30] in water. In this system, the polystyrene blocks form the micelle core surrounded by polymethacrylic acid corona. The amount solubilized was measured for 18 different organic molecules including aliphatic, cyclic and aromatic hydrocarbons, chlorinated hydrocarbons, and esters in two block copolymers, SA-23 (PS₃₁₇PMA₂₅₆) and SA-24 (PS₂₅₆PMA₂₀₉) having different block sizes and composition. The numerical solubilization data are summarized in Table S3 in the Supplemental Information. In Fig. 5, the Flory interaction parameters for polystyrene-solubilize have been correlated against the mass solubilization ratio (mass of solubilize to mass of copolymer) for the two block copolymers. The correlation again confirms the controlling influence of the core block-solubilize interaction parameter.

In contrast, the solubilization data in Table 8 for the surfactant SDS shows that the amount of solubilization increases with increasing χ_{AO} (calculated using the solubility parameters as described before). Obviously, the Flory parameter bears no correlation to MSR in this case. This behavior can be traced to the smaller aggregate sizes and the relatively more prominent role for the interfacial interactions in the case of SDS micelles. Consequently, the volume-interfacial activity parameter exhibits a better correlation for SDS micelles. The block copolymer micelles have core radii in the range of at least few nm and certainly more than the 1 to 2 nm typical of surfactant micelles. Consequently, the swelling of the core block by the solubilize makes an important contribution to the free energy, in contrast to the interfacial free energy effect discussed for the surfactant micelle. The interfacial energy effect is still relevant for the block copolymers but the controlling influence of the interface interactions vs the core interactions is determined by

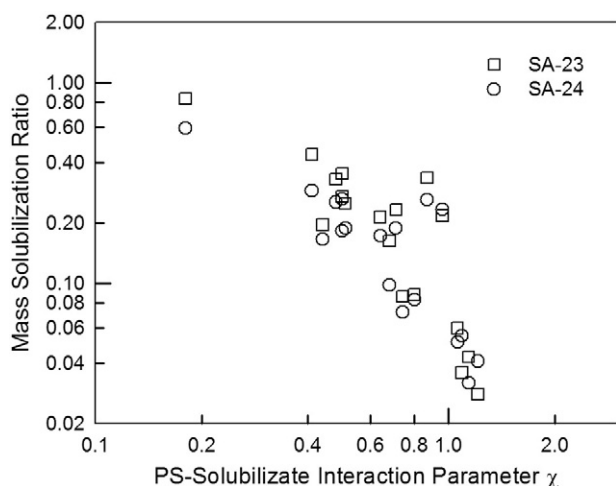


Fig. 5. Measured mass solubilization ratio [30] for various organic molecules in micelles formed of polystyrene-polymethacrylic acid (PS-PMA) block copolymer. The two block copolymers represent differing molecular weights and block compositions. The numerical data used for the plot are listed in Table S3 of the Supplemental Information.

how large the core forming solvophobic block is and the corresponding core dimensions. The larger these values are, the dominant control is exercised by the bulk interactions within the core. When the core size is smaller, both the core interactions and interface interactions would have competing control.

5. Conclusions and perspectives

5.1. Interplay of surfactant and block copolymer models

Although surfactants and block copolymers exhibit analogous self-assembly behavior, theoretical models describing them have evolved independent of one another, emphasizing mutually exclusive molecular features. In the Tanford model for surfactant micelle, the balancing of surfactant head group repulsions against the interfacial energy determines the equilibrium properties of the aggregate. Noticeably absent was any influence attributed to the hydrophobic tail over the aggregate size and shape. In the de Gennes model for block copolymer micelle, the micelle characteristics are determined by the balancing of elastic deformation of the solvophobic block against the interfacial energy. The solvophilic block interactions (which are the analog of the surfactant head group interactions) play no role in determining the micelle characteristics. By incorporating the mutually neglected free energy contributions between these two theoretical models, we can have a unitary theory applicable to both surfactants and block copolymers. The incorporation of surfactant tail deformation free energy by borrowing from the block copolymer model has led to more accurate predictions of the critical micelle concentration and micelle characteristics for many classical surfactants [16,31]. Similarly, the incorporation of solvophilic block interactions by borrowing from the surfactant model provides predictions about block copolymer micelles that are consistent with recent experiments focusing on the solvophilic block effect [32,33]. The interplay of ideas from surfactants and block copolymer models have also influenced our understanding of shape transitions of surfactant and block copolymer aggregates and the solubilization behavior of the two kinds of amphiphiles. Specifically we show how aggregate shape transitions are controlled by molecular packing for surfactants because of the constraint imposed by the limited extended length of the surfactant tail. In contrast, the free energy criteria completely controls the aggregate shape transitions for block copolymers since there are no packing constraints imposed by the solvophobic block. Further, we show that solubilization in surfactant micelles is controlled by interfacial interactions at micelle surface because of the relatively small core dimension while in block copolymer micelles it is controlled by bulk interactions in the core because of the typical larger core dimension. Overall, the interplay of ideas applied to surfactants and block copolymers have contributed to the creation of useful predictive self-assembly models describing both classes of amphiphiles.

5.2. Recent progress in adaptation of models for diverse self-assembly phenomena

The free energy models evolved by combining critical features from surfactant and block copolymer theories have been adapted and applied to many diverse problems of self-assembly and have been demonstrated to produce quantitatively reliable predictions. We have adapted the free energy models to predict the formation of mixed micelles exhibiting ideal and non-ideal mixing behavior [16,34], solubilization and solubilize-induced shape transition of aggregates [16,35], formation of giant rodlike micelles from surfactants, surfactant mixtures, and surfactant-alcohol mixtures [36], aggregation of Gemini surfactants [37], surfactant aggregation in polar solvents [38] and in aqueous-organic mixed solvents [39], surfactant aggregation at hydrophobic [40] and hydrophilic solid surfaces [41] and the formation of droplet and bicontinuous type microemulsions [42]. Blankschtein group has adopted alternate approaches to estimating the tail packing free energy

contribution and have constructed quantitatively accurate predictive free energy models for nonionic, ionic and zwitterionic surfactants [43–45], surfactant mixtures [46–48], counterion effects in ionic surfactants [49,50], fluorocarbon surfactants [51] and fluorocarbon-hydrocarbon surfactant mixtures [52].

5.3. Emergence of novel amphiphiles and future challenges to modeling

The free energy models discussed in this review now face the challenge of being adapted and applied to emerging novel amphiphiles that combine biological or inorganic elements or nanoparticles into classical surfactant, lipid or polymer structures. One example is the DNA-programmed lipid consisting of two alkyl hydrophobic tails, linked covalently to the 5'-termini of a single-stranded DNA (ssDNA) oligonucleotide that functions as hydrophilic head group [53]. The DNA hybridization generates "new" surfactants and by manipulating the size, shape, and charge of the polar head group of the surfactant molecule via DNA hybridization and displacement cycles, one could change the aggregation patterns. Another example is surfactants containing a purely inorganic multinuclear head group of the polytungstate type R-[PW₁₁O₃₉]₃ [54]. Such polyoxometalate (POM) surfactants self-assemble into micelles and lyotropic phases and can simultaneously play the conventional role of surfactant such as for emulsification as well as act as a catalyst for a chemical reaction. Another class of amphiphiles are those incorporating peptides such as the amphiphiles with a hydrophobic small polymer tail and multiple hydrophilic peptides as the head group [55]. The peptides were selected to be substrates for cancer-associated proteins and were amenable to proteolysis. Since each peptide in the head group can be chemically modified by proteolysis by a specific enzyme, an enzyme-responsive switching of the morphology of the micelles could be realized. The ability to program the nature of micelle responses to disease-associated enzymes, through peptide design, has implications for *in vivo* delivery and detection methods. Tirrell and coworkers have investigated [56] peptide amphiphiles that form worm-like micelles resembling nanofibers, that are viewed as potential synthetic extracellular matrix materials for tissue engineering and regenerative medicine. A general approach to dynamically constructing and destroying amphiphiles has been proposed [57] by Montenegro et al. These dynamic amphiphiles have a charged head, a hydrophobic tail, and a dynamic connector or "bridge". The dynamic covalent bonds of bridges, formed with, for example, hydrazones, disulfides or oximes, are weaker than common covalent bonds but stronger than non-covalent interactions, such as hydrogen bonds. Because of the dynamic nature of their bridges, dynamic amphiphiles can be formed, modified and destroyed, *in situ*, depending on environmental conditions. Cheng and collaborators have introduced the concept of "giant surfactants" consisting of compact and rigid nanoparticles as head group and flexible polymer chains as tail [58,59]. Examples include giant surfactants based on functionalized fullerene, polyhedral oligomeric silsesquioxanes (POSS), and polyoxometalate (POM) derivatives, with variable surface functionalities. The giant surfactants capture the essential features of small molecular weight classical surfactants but with sizes comparable to block copolymers.

Existing free energy models of surfactants and block copolymers need to be adapted and extended to account for interactional terms connected to novel head groups such as peptides, oligonucleotides, POSS, POM, etc., and also to account for novel hydrophobic tails such as hydrophobic peptides, fullerenes, etc., in order to quantitatively describe the wide pattern of aggregation observed. The design of such novel amphiphiles incorporating responsiveness and programmability and the ability to combine organic, inorganic and biological moieties within a single molecular structure, makes this area a very interesting and fertile field of research for years to come. The novel amphiphiles make possible entirely new areas of applications in materials science and nanomedicine, far beyond the traditional colloidal applications of surfactants and block copolymers.

Conflict of interest

No conflict of interest.

Acknowledgements

Professor Ruckenstein has collaborated in many parts of the work discussed here as can be inferred from the cited references, and the author has benefited from numerous discussions with him. The predictive theories described in this review were developed during the author's tenure at The Pennsylvania State University. Key contributions of author's past graduate students at Penn State, Kailasam Ganesh, Mark Chaiko and Maureen Barry are acknowledged and referenced in the text. Support from Natick Soldier Research, Development and Engineering Center is acknowledged for continuing theoretical studies of self-assembly and the preparation of this manuscript.

Appendix A. Supplementary data

Supplementary data to this article can be found online at <http://dx.doi.org/10.1016/j.cis.2016.12.001>.

References

- [1] Tanford C. *The hydrophobic effect*. Wiley; 1973.
- [2] Israelachvili JN, Mitchell JD, Ninham BW. *J Chem Soc Faraday Trans 2* 1976;72:1525.
- [3] Meier DJ. *J Polym Sci C* 1969;26:81.
- [4] Meier DJ. *Polym Prepr* 1970;11:400.
- [5] Helfand E, Tagami Y. *J Polym Sci B* 1971;9:741.
- [6] Helfand E, Sapse AM. *J Chem Phys* 1975;62:1327.
- [7] de Gennes PG. In: Liebert J, editor. *Solid state physics*. Academic Press; 1978. p. 1–18 [Suppl. 14].
- [8] Leibler L, Orland H, Wheeler JC. *J Chem Phys* 1983;79:3550.
- [9] Noolandi J, Hong KM. *Macromolecules* 1983;16:1443.
- [10] Whitmore D, Noolandi J. *Macromolecules* 1985;18:657.
- [11] Tanford C. *J Phys Chem* 1974;78:2469.
- [12] Daoud M, Cotton JP. *J Phys* 1982;43:531.
- [13] Zhulina YB, Birshtein TM. *Polym Sci USSR* 1985;27:570.
- [14] Halperin A. *Macromolecules* 1987;20:2943.
- [15] Nagarajan R, Ganesh K. *J Chem Phys* 1993;98:7440.
- [16] Nagarajan R, Ruckenstein E. *Langmuir* 1991;7:2934.
- [17] Semenov AN. *Sov Phys JEIP* 1985;61:733.
- [18] Nagarajan R, Ganesh K. *J Chem Phys* 1989;90:5843.
- [19] Nagarajan R, Ganesh K. *Macromolecules* 1989;22:4312.
- [20] Nagarajan R, Ganesh K. *J Colloid Interface Sci* 1996;184:489.
- [21] Bahadur P, Sastry NV, Marti S, Riess G. *Colloids Surf* 1985;16:337.
- [22] Nagarajan R. In: Nagarajan R, editor. *Amphiphiles: Molecular assembly and applications*, American Chemical Society; 2010 [Chapter 1, pp.].
- [23] Nagarajan R. *Langmuir* 2002;18:31.
- [24] Smart T, Lomas H, Massignani M, Flores-Merino MV, Perez LR, Battaglia G. *Nano Today* 2008;3:38.
- [25] Holder SJ, Sommerdijk NAJM. *Polym Chem* 2011;2:1018.
- [26] Lettow JS, Lancaster TM, Glinka CJ, Ying JY. *Langmuir* 2005;21:5738.
- [27] Chaiko MA, Nagarajan R, Ruckenstein E. *J Colloid Interface Sci* 1984;99:168.
- [28] Nagarajan R, Barry M, Ruckenstein E. *Langmuir* 1986;1:210.
- [29] Flory PJ. *Principles of polymer chemistry*. Cornell University Press; 1962.
- [30] Tian M, Arca E, Tuzar Z, Webber SE, Munk P. *J Polym Sci B* 1995;33:1713.
- [31] Nagarajan R. In: Esumi K, Ueno M, editors. *Structure-performance relationships in surfactants*. Marcel Dekker; 2003. p. 1–110 [Chapter 1].
- [32] Jensen GV, Shi Q, Deen GR, Almdal K, Pedersen JS. *Macromolecules* 2012;45:430.
- [33] Caba BL, Zhang Q, Carroll MRJ, Woodward RC, St. Pierre TG, Gilbert EP, et al. *J Colloid Interface Sci* 2010;344:81.
- [34] Nagarajan R. In: Holland PM, Rubingh DN, editors. *Mixed surfactant systems*. American Chemical Society; 1992. p. 54–95 [Chapter 4].
- [35] Nagarajan R, Ruckenstein E. In: Sengers JV, Kayser RF, Peters CJ, White Jr HJ, editors. *Equations of state for fluids and fluid mixtures*. Elsevier; 2000. p. 589–749 [Chap. 15].
- [36] Nagarajan R. In: Zana R, Kaler E, editors. *Giant micelles. Properties and applications*. Taylor and Francis; 2007. p. 1–40 [Chapter 1].
- [37] Camesano TA, Nagarajan R. *Colloids Surf A* 2000;167:165.
- [38] Nagarajan R, Wang CC. *J Colloid Interface Sci* 1996;178:471.
- [39] Nagarajan R, Wang CC. *Langmuir* 2000;16:5242.
- [40] Johnson RA, Nagarajan R. *Colloids Surf A* 2000;167:31.
- [41] Johnson RA, Nagarajan R. *Colloids Surf A* 2000;167:21.
- [42] Nagarajan R, Ruckenstein E. *Langmuir* 2000;16:6400.
- [43] Puvvada S, Blankschtein D. *J Chem Phys* 1990;92:3710.
- [44] Naor A, Puvvada S, Blankschtein D. *J Phys Chem* 1992;96:7830.
- [45] Zoeller N, Lue L, Blankschtein D. *Langmuir* 1997;13:5258.
- [46] Puvvada S, Blankschtein D. *J Phys Chem* 1992;96:567.

- [47] Yuet PK, Blankschtein D. *Langmuir* 1996;12:3802.
- [48] Shiloach A, Blankschtein D. *Langmuir* 1998;14:1618.
- [49] Srinivasan V, Blankschtein D. *Langmuir* 2003;19:9932.
- [50] Srinivasan V, Blankschtein D. *Langmuir* 2003;19:9946.
- [51] Srinivasan V, Blankschtein D. *Langmuir* 2005;21:1647.
- [52] Iyer J, Blankschtein D. *J Phys Chem B* 2014;118:2377.
- [53] Thompson MP, Chien MP, Ku TH, Rush AM, Gianneschi NC. *Nano Lett* 2010;10:2690.
- [54] Landsmann S, Lizandara-Pueyo C, Polarz S. *J Am Chem Soc* 2010;132:5315.
- [55] Ku TH, Chien MP, Thompson MP, Sinkovits RS, Olson NH, Baker TS, et al. *J Am Chem Soc* 2011;133:8392.
- [56] Shimada T, Sakamoto N, Motokawa R, Koizumi S, Tirrell M. *J Phys Chem B* 2012;116:240.
- [57] Montenegro J, Bang EK, Sakai N, Matile S. *Chem A Eur J* 2012;18:10436.
- [58] Yu X, Li Y, Dong XH, Yue K, Lin Z, Feng X, et al. *J Polym Sci B* 2014;52:1309.
- [59] Lin Z, Lu P, Hsu CH, Sun J, Zhou Y, Huang M, et al. *Macromolecules* 2015;48:5496.